

## Sol-Gel Synthesis of $\text{Ca}_{2.8}\text{Pr}_{0.2}\text{Co}_4\text{O}_9$ Powders with Thermal and Structural Characterization

\*<sup>1</sup>Enes Kilinc, <sup>2</sup>M. Abdullah Sari, <sup>1</sup>Fatih Uysal, <sup>3,4,5</sup>Erdal Celik and <sup>1</sup>Huseyin Kurt

<sup>1</sup>Faculty of Engineering, Department of Mechanical Engineering, Karabuk University, Karabuk, Turkey

<sup>2</sup>The Graduate School of Natural and Applied Sciences, Department of Metallurgical and Materials Engineering, Dokuz Eylul University, Izmir, Turkey

<sup>3</sup>Center for Production and Application of Electronic Materials (EMUM), Dokuz Eylul University, Izmir, Turkey

<sup>4</sup>Faculty of Engineering, Department of Metallurgical and Materials Engineering, Dokuz Eylul University, Izmir, Turkey

<sup>5</sup>The Graduate School of Natural and Applied Sciences, Department of Nanoscience & Nanoengineering, Dokuz Eylul University, Izmir, Turkey

### Abstract

In this paper,  $\text{Ca}_{2.8}\text{Pr}_{0.2}\text{Co}_4\text{O}_9$  powders were synthesized by sol-gel method and thermal and structural characterization of the powders were systematically examined for high temperature thermoelectric generator applications. Solution characteristics of precursors were examined by Turbidity and pH measurements using a turbidimeter and a pH meter. Differential Thermal Analysis-Thermogravimetry (DTA-TG) was used to specify appropriate thermal regime of the powders for calcination process. Chemical structure and reaction type of intermediate temperature products were defined by Fourier Transform Infrared (FTIR) Spectroscopy. Structural properties of the powders were implemented by X-ray Diffraction (XRD) and X-ray Photoelectron Spectroscopy (XPS) was used to specify chemical composition and empirical formula of the elements existed within the powders. Drying, oxidation and phase transformation temperatures of the powders were optimized according to the DTA-TG and FTIR results. Considering the DTA curve, endothermic and exothermic reactions took place between temperature interval of 270 °C and 480 °C due to drying process at 200 °C. In addition, phase formation peaks of  $\text{Ca}_{2.8}\text{Pr}_{0.2}\text{Co}_4\text{O}_9$  powders can be observed in the XRD study. It can be seen from the phase spectrum that  $2\theta$  peaks correspond to the literature and coincide with typical  $\text{Ca}_3\text{Co}_4\text{O}_9$  peaks.

**Key words:** Sol-gel processes, photoelectron spectroscopies, thermal analysis, X-ray diffraction.

### 1. Introduction

Thermoelectric (TE) materials have attracted a great deal of attention by converting heat energy into electrical energy directly for thermoelectric power generation applications [1]. Recently, TE oxides became advantageous over alloy based intermetallic compounds in terms of high temperature stability, cost of starting materials, easy manufacturing and high temperature application areas [2]. Having looked at oxide TE materials,  $\text{Ca}_3\text{Co}_4\text{O}_9$  [3] and ZnO [4] have become important candidates for p- and n-type oxide TE materials with high figure of merit (ZT) values at high temperatures. In the past decade, many methods including doping have been used to improve their TE properties. Doping methods are the major approach to improve ZT of bulk materials [5]. Through these studies, ZT values of bulk oxide TE materials have reached to 0.5 at 1000 K and

\*Corresponding author: Address: Karabuk Universitesi, Muhendislik Fakultesi, Makina Muhendisligi Bolumu, Oda No: 348, 78050, Karabuk, Turkey. E-mail address: eneskilinc@karabuk.edu.tr.

0.65 at 1247 K for p-type  $\text{Ca}_{2.7}\text{Ag}_{0.3}\text{Co}_4\text{O}_9/\text{Ag}$ -10 wt.% composite [6] and n-type  $\text{Zn}_{0.96}\text{Al}_{0.02}\text{Ga}_{0.02}\text{O}$  [7], respectively.

Over the past decades, many synthesis methods have been used to synthesize  $\text{Ca}_3\text{Co}_4\text{O}_9$  and ZnO powders such as solid state reaction method [8], self-ignition method [9], combustion synthesis method [10], and sol-gel method [11]. Between these methods, sol-gel synthesis has some advantages among them as better stoichiometry control and homogeneity, lower reaction temperatures, easy fabrication and opportunity of using high-purity precursors [12].

In this study,  $\text{Ca}_3\text{Co}_4\text{O}_9$  was doped with rare earth element Pr on the Ca side using sol-gel synthesis for thermoelectric generator (TEG) applications. Synthesis and characterization of  $\text{Ca}_{2.8}\text{Pr}_{0.2}\text{Co}_4\text{O}_9$  were performed systematically using Ca, Pr and Co based precursors, and solutions of these precursors were prepared with their solvents and chelating agents. This paper includes characterization methods to identify solution characteristics, process regime, structural properties and elemental composition of the powders. Within this scope, solution characteristics of the precursors were determined by pH and turbidity measurements. Thermal properties of the powders were characterized by Differential Thermal Analysis-Thermogravimetry (DTA-TG) in order to obtain appropriate calcination regime and Fourier Transform Infrared (FTIR) Spectroscopy was used to define chemical structure and reaction type of intermediate temperature products. Structural analysis of the  $\text{Ca}_{2.8}\text{Pr}_{0.2}\text{Co}_4\text{O}_9$  powders was carried out using X-ray Diffraction (XRD) and results were compared with literature. In addition, X-ray Photoelectron Spectroscopy (XPS) was used to specify elemental composition and empirical formula of the elements within the powders.

## 2. Materials and Method

First of all, all the precursors were dissolved in their solvents and solutions of the precursors were prepared adding their chelating agents. Characteristics of the solutions were investigated by pH and turbidity measurements. After gelation process, xerogel was dried at 200 °C for 2 h and powders were obtained. Hereafter, DTA-TG analysis were achieved to specify thermal attributes of the powders and XRD analysis were managed to state structural analysis. Finally, elemental composition of elements within the powders was assigned by XPS.

In this study,  $\text{Ca}_{2.8}\text{Pr}_{0.2}\text{Co}_4\text{O}_9$  powders were synthesized using sol-gel method. Calcium nitrate tetra hydrate (99%, Alfa Aesar), praseodymium (III) nitrate hydrate (99.9%, Alfa Aesar) and cobalt (II) nitrate hexahydrate (ACS, Alfa Aesar) were used in stoichiometric ratios as starting materials. Distilled water was used as the solvent to dissolve each precursor having fully dispersed and homogenous solutions. Amounts of the precursors, solvent and chelating agent were given in **Table 1** used for the synthesis of 0.02 mole  $\text{Ca}_{2.8}\text{Pr}_{0.2}\text{Co}_4\text{O}_9$ . After obtaining separate solutions of the precursors, the solutions were mixed and magnetically stirred at 100 °C to obtain final homogeneous solution and citric acid monohydrate was added as the chelating agent to accelerate xerogel formation. After gelation, obtained xerogel was dried at 200 °C for 2 h to remove moisture and undesired gases.

**Table 1.** Stoichiometric ratios used for 0.02 mole of  $\text{Ca}_{2.8}\text{Pr}_{0.2}\text{Co}_4\text{O}_9$  powders.

Precursors	Molecular Weight (g/mole)	Amount
Calcium nitrate tetra hydrate	236.15	13.2244 g
Praseodymium (III) nitrate hydrate	291.04	23.2832 g
Cobalt (II) nitrate hexahydrate	326.92	1.3077 g
Distilled water	18	200 ml
Citric acid monohydrate	210.14	4.2028 g

Solution characteristics of the solutions were specified by a turbidimeter and a pH meter, respectively, maintaining turbidity and pH values. A VELP TB1 model turbidimeter was used to measure the turbidity value of the solutions with a measurement range of 0-1000 ntu (nephelometric turbidity unit). Acidic and basis characteristics of the final solution was determined by measuring its pH value with a WTW Inolab pH 720 model pH meter after the dispersion process.

A Perkin Elmer STA 6000 model DTA-TG instrument was used to identify thermal behavior of the dried powders from ambient temperature to 900 °C in air atmosphere with a heating rate of 10 °C/min. Solution evaporation, decomposition and phase formation of the powders were stated as a result of DTA-TG analysis. Prior to XRD analysis, the dried powders were calcined at 800 °C for 2 h resulting as final  $\text{Ca}_{2.8}\text{Pr}_{0.2}\text{Co}_4\text{O}_9$  powders. XRD pattern of the final powders was identified by a Thermo Scientific ARL model X-ray diffractometer using  $\text{Cu K}_\alpha$  irradiation (wavelength,  $\lambda = 1.540562 \text{ \AA}$ ) in the range of  $5^\circ \leq 2\theta \leq 90^\circ$  at a speed of  $2^\circ/\text{min}$ . Elemental composition and element ratios of the powders were described using a A Thermo Scientific K-Alpha model XPS device with an  $\text{Al K}_\alpha$  X-ray source between 0-1350 eV energy range.

### 3. Results and Discussion

It is important to specify if powder precursors are dissolved completely in solutions in terms of obtaining homogeneous solutions. Within this context, turbidity measurements are performed by inspecting ntu values of the solutions in the range of 0-1000 ntu. A homogeneous solution has been formed if the turbidity value is reputed to be closer to 0, and powder precursors have not been dissolved entirely in solutions if the turbidity value is measured closer to 1000 [13]. In addition, gel formation is affected by the pH value of the solutions and the pH value ought to be regarded during solution preparation. In this work, turbidity and pH values of the prepared solution were found as 0.36 ntu and 1.19, respectively, meaning that the precursors were dissolved very well in the solution and the solution showed acidic characteristics forming a branched structure during the gelation process.

DTA-TG analysis was applied to the  $\text{Ca}_{2.8}\text{Pr}_{0.2}\text{Co}_4\text{O}_9$  powders dried at 200 °C for 2 h in air with a heating rate of 10 °C per minute in air atmosphere until 900 °C and the results are shown in **Fig. 1**. Endothermic and exothermic reactions occur at the temperature range of 270 °C and 480 °C with reference to DTA curve in the figure. Exothermic peak between 270 °C and 300 is related to

burning out of organic residuals containing C based materials. At the same temperature interval, a weight loss of 10% is stated from TG curve due to removal of organic groups. Endothermic peak between temperatures of 440 °C and 480 °C is regarded to oxidation of Ca, Pr, and Co. A significant weight loss of approximately 30% on the TG curve is observed due to these peaks. Phase formation of  $\text{Ca}_{2.8}\text{Pr}_{0.2}\text{Co}_4\text{O}_9$  starts after 480 °C according to the DTA curve and small weight losses were observed depending on the phase formation.

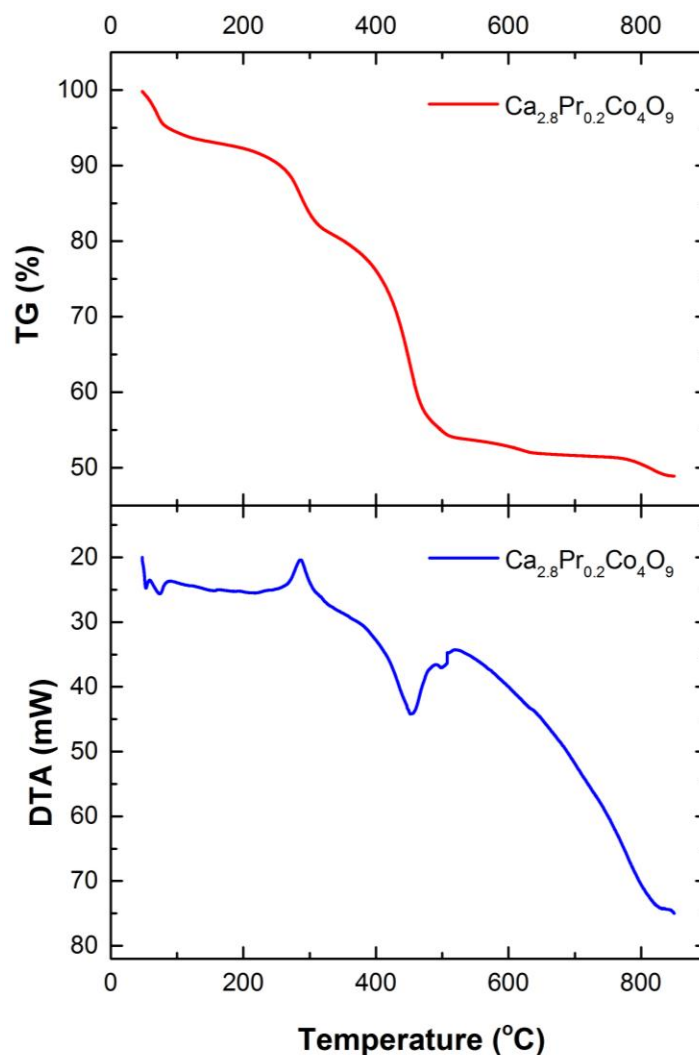


**Fig. 1.** DTA and TG curves of  $\text{Ca}_{2.8}\text{Pr}_{0.2}\text{Co}_4\text{O}_9$  powders dried at 200 °C in air.

XRD pattern of  $\text{Ca}_{2.8}\text{Pr}_{0.2}\text{Co}_4\text{O}_9$  powders manufactured by sol-gel method is shown in **Fig. 2**. Formation of crystalline structure for  $\text{Ca}_{2.8}\text{Pr}_{0.2}\text{Co}_4\text{O}_9$  particles was depicted with sharp diffraction peaks.  $2\theta$  peaks at  $16.54^\circ$ ,  $24.86^\circ$ ,  $30.30^\circ$ ,  $33.38^\circ$ ,  $37.22^\circ$ ,  $39.56^\circ$ ,  $43.46^\circ$ ,  $48.68^\circ$ , and  $55.46^\circ$  seen from the phase spectrum correspond to typical  $\text{Ca}_3\text{Co}_4\text{O}_9$  peaks and are agreeable with the literature [14]. Any other phases were not observed in the XRD detection. In addition, average crystalline size of  $\text{Ca}_{2.8}\text{Pr}_{0.2}\text{Co}_4\text{O}_9$  particles were determined using the intensities of the primary peaks of

reflection at  $2\theta=33.38^\circ$  by the Debye-Scherer equation [15] which is given as  $D = 0.9\lambda/\beta\cos\theta$ . Here,  $D$  is the average crystalline size,  $\lambda$  is the X-ray wavelength,  $\beta$  is the full width at half the maximum intensity, and  $\theta$  is the Bragg's diffraction angle. Average crystalline size of the  $\text{Ca}_{2.8}\text{Pr}_{0.2}\text{Co}_4\text{O}_9$  particles was calculated as 27.6 nm using Debye-Scherer equation.

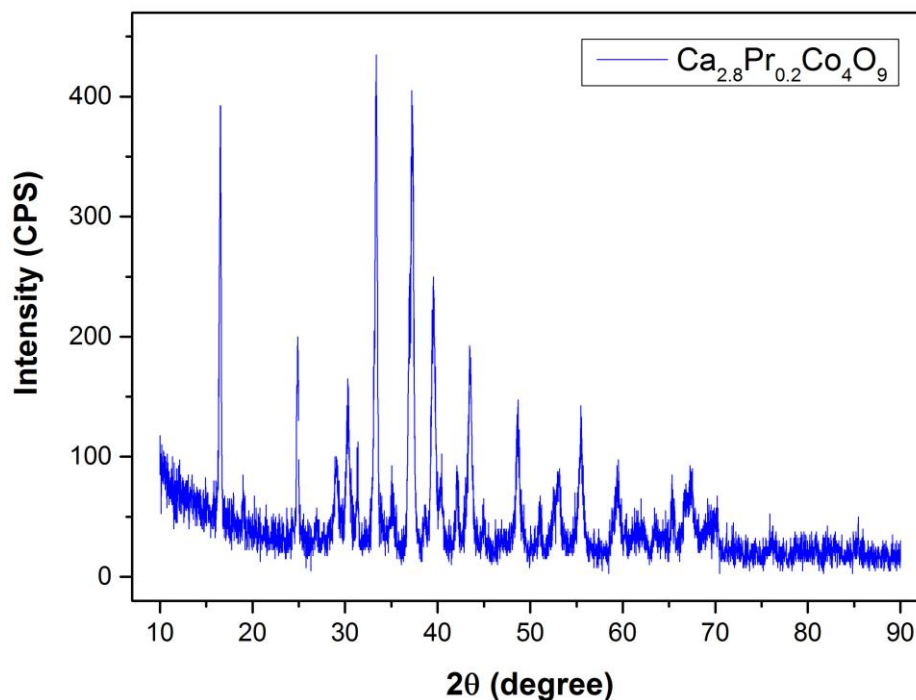


**Fig. 2.** XRD spectra of  $\text{Ca}_{2.8}\text{Pr}_{0.2}\text{Co}_4\text{O}_9$  powders calcined at  $800^\circ\text{C}$  for 2 h in air.

A wide scan XPS spectra of  $\text{Ca}_{2.8}\text{Pr}_{0.2}\text{Co}_4\text{O}_9$  powders was evaluated within the range of 0-1350 eV with an energy step size of 1.0 eV. According to in **Fig. 3**. Sharp peaks seen in the XPS spectra confirm that elements of Ca, Pr, Co, and O exist within the powder sample corresponding with the peaks. In addition, peaks corresponding to C and Cl are also detected in the spectra. Existence of Cl is the result of distilled water used to dissolve the precursors and C is the result of reaction with  $\text{CO}_2$  in air. **Table 3** gives elemental analysis and quantification of  $\text{Ca}_{2.8}\text{Pr}_{0.2}\text{Co}_4\text{O}_9$  powders including binding energies (BE) in eV with their corresponding full-width at half maximum (FWHM). Elemental analysis from XPS shows that  $\text{Ca}_{2.8}\text{Pr}_{0.2}\text{Co}_4\text{O}_9$  powders consist of 14.25% Ca, 38.24% O, 7.21% Co, and 0.46% Pr. It can be noticed from the table that components of Ca 2p, O 1s, Co 2p, and Pr 4d are formed with binding energies of 346.21 eV, 530.05 eV, 780.23 eV, and 115.81 eV, respectively. Although effect of Pr doping cannot be detected in the XRD pattern, presence of Pr dopant can be detected in the XPS spectra. Hence, doping of Pr into  $\text{Ca}_3\text{Co}_4\text{O}_9$  was successfully accomplished.

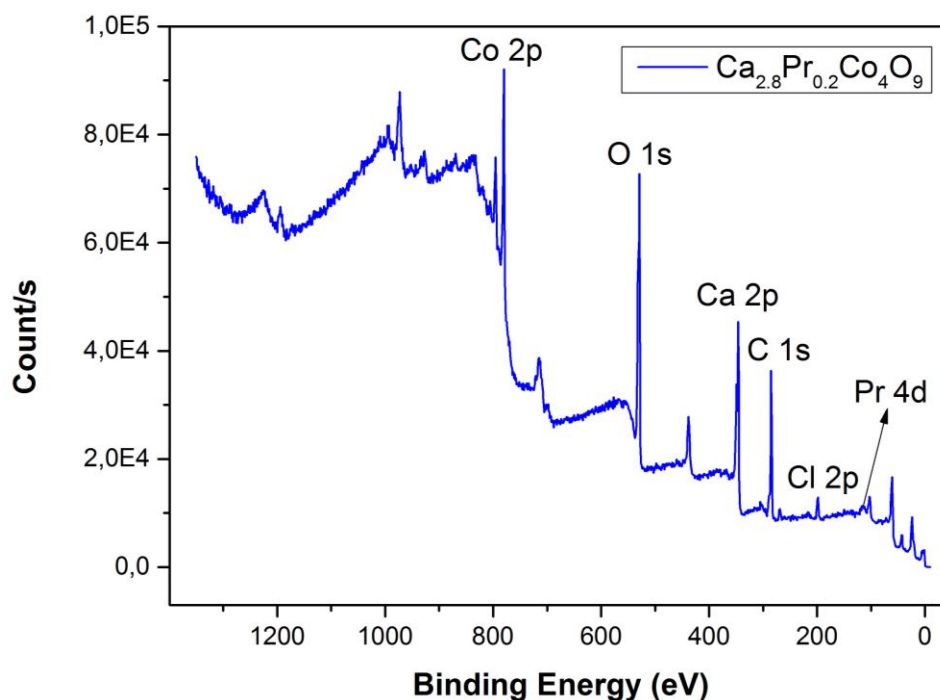


Fig. 3. Wide survey XPS spectra of  $\text{Ca}_{2.8}\text{Pr}_{0.2}\text{Co}_4\text{O}_9$  powders.

Table 3. Elemental analysis and quantification of  $\text{Ca}_{2.8}\text{Pr}_{0.2}\text{Co}_4\text{O}_9$  powders.

Peak	Position BE (eV)	FWHM (eV)	Area (cps eV)	Amount (%)
Ca 2p	346.21	3.368	143301.59	14.25
O 1s	530.05	4.451	199972.85	38.24
Co 2p	780.23	3.072	205702.10	7.21
Pr 4d	115.81	3.811	7567.86	0.46

## Conclusions

This study contains successfully synthesis and characterization of  $\text{Ca}_{2.8}\text{Pr}_{0.2}\text{Co}_4\text{O}_9$  powders for high temperature thermoelectric applications using sol-gel method. Solution characteristics were specified with the turbidity and pH measurements exhibiting that the precursors were dissolved excellently in the solutions and the gelation process was victorious. As a result of thermal analysis, endothermic and exothermic reactions occurred at the temperature range of 270 °C and 480 °C with reference to DTA curve for the  $\text{Ca}_{2.8}\text{Pr}_{0.2}\text{Co}_4\text{O}_9$  powders dried at 200 °C. At the temperature interval of 270 °C - 300 °C, a weight loss of 10% is stated from TG curve due to removal of organic groups. A significant weight loss of approximately 30% on the TG curve is observed between 440 °C - 480 °C due to oxidation peaks of Ca, Pr, and Co. Lastly, phase formation of  $\text{Ca}_{2.8}\text{Pr}_{0.2}\text{Co}_4\text{O}_9$  starts after 480 °C according to the DTA curve. Formation of crystalline structure for  $\text{Ca}_{2.8}\text{Pr}_{0.2}\text{Co}_4\text{O}_9$  particles was depicted with sharp diffraction peaks in the XRD pattern

corresponding to typical  $\text{Ca}_3\text{Co}_4\text{O}_9$  peaks compatible with the literature. In addition, average crystalline size of the  $\text{Ca}_{2.8}\text{Pr}_{0.2}\text{Co}_4\text{O}_9$  particles was calculated as 27.6 nm using Debye-Scherrer equation. Sharp peaks seen in the wide survey XPS spectra confirm that elements of Ca, Pr, Co, and O exist within the powder sample. Although effect of Pr doping cannot be detected in the XRD pattern, presence of Pr dopant can be detected in the XPS spectra. Hence, doping of Pr into  $\text{Ca}_3\text{Co}_4\text{O}_9$  was successfully accomplished.

## Acknowledgements

This work was supported by the Scientific and Technological Research Council of Turkey (TUBITAK) in Turkey under Project No. 115M579. We would like to thank the Center for Production and Application of Electronic Materials (EMUM) in Dokuz Eylul University in Izmir, Turkey for research collaboration.

## References

1. Garcia-Canadas J, Min G (2014) Multifunctional probes for high-throughput measurement of Seebeck coefficient and electrical conductivity at room temperature. *The Review of scientific instruments* 85 (4):043906. doi:10.1063/1.4871553
2. Funahashi R, Mikami M, Mihara T, Urata S, Ando N (2006) A portable thermoelectric-power-generating module composed of oxide devices. *Journal of Applied Physics* 99 (6):066117. doi:10.1063/1.2180449
3. Song Y, Sun Q, Zhao L, Wang F, Jiang Z (2009) Synthesis and thermoelectric power factor of  $(\text{Ca}_{0.95}\text{Bi}_{0.05})_3\text{Co}_4\text{O}_9/\text{Ag}$  composites. *Materials Chemistry and Physics* 113 (2-3):645-649. doi:10.1016/j.matchemphys.2008.08.029
4. Han L, Nong NV, Hung LT, Holgate T, Pryds N, Ohtaki M, Linderoth S (2013) The influence of  $\alpha$ - and  $\gamma$ - $\text{Al}_2\text{O}_3$  phases on the thermoelectric properties of Al-doped ZnO. *Journal of Alloys and Compounds* 555:291-296. doi:10.1016/j.jallcom.2012.12.091
5. Alam H, Ramakrishna S (2013) A review on the enhancement of figure of merit from bulk to nano-thermoelectric materials. *Nano Energy* 2 (2):190-212. doi:10.1016/j.nanoen.2012.10.005
6. Wang Y, Sui Y, Cheng J, Wang X, Su W (2009) Comparison of the high temperature thermoelectric properties for Ag-doped and Ag-added  $\text{Ca}_3\text{Co}_4\text{O}_9$ . *Journal of Alloys and Compounds* 477 (1-2):817-821. doi:10.1016/j.jallcom.2008.10.162
7. Van Nong N, Pryds N, Linderoth S, Ohtaki M (2011) Enhancement of the thermoelectric performance of p-type layered oxide  $\text{Ca}_3\text{Co}_4\text{O}_{9+\delta}$  through heavy doping and metallic nanoinclusions. *Advanced materials* 23 (21):2484-2490. doi:10.1002/adma.201004782
8. Chen C, Zhang T, Donelson R, Chu D, Tian R, Tan TT, Li S (2014) Thermopower and chemical stability of  $\text{Na}_{0.77}\text{CoO}_2/\text{Ca}_3\text{Co}_4\text{O}_9$  composites. *Acta Materialia* 63:99-106. doi:10.1016/j.actamat.2013.10.011
9. Su H, Jiang Y, Lan X, Liu X, Zhong H, Yu D (2011)  $\text{Ca}_{3-x}\text{Bi}_x\text{Co}_4\text{O}_9$  and  $\text{Ca}_{1-y}\text{Sm}_y\text{MnO}_3$  thermoelectric materials and their power-generation devices. *physica status solidi (a)* 208 (1):147-155. doi:10.1002/pssa.201026347

10. Park K, Hwang HK, Seo JW, Seo WS (2013) Enhanced high-temperature thermoelectric properties of Ce- and Dy-doped ZnO for power generation. *Energy* 54:139-145. doi:10.1016/j.energy.2013.03.023
11. Nan SW, J.; Deng, Y.; Nan, C.W. (2003) Synthesis and thermoelectric properties of  $(\text{Na}_x\text{Ca}_{1-x})_3\text{Co}_4\text{O}_9$  ceramics. *Journal of the European Ceramic Society* 23:859-863
12. Goktas A, Mutlu IH, Yamada Y, Celik E (2013) Influence of pH on the structural optical and magnetic properties of  $\text{Zn}_{1-x}\text{Mn}_x\text{O}$  thin films grown by sol-gel method. *Journal of Alloys and Compounds* 553:259-266. doi:10.1016/j.jallcom.2012.11.097
13. Celik E, Aybarc U, Ebeoglugil MF, Birlik I, Culha O (2009) ITO films on glass substrate by sol-gel technique: synthesis, characterization and optical properties. *Journal of Sol-Gel Science and Technology* 50 (3):337-347. doi:10.1007/s10971-009-1931-4
14. Liu HQ, Zhao XB, Zhu TJ, Song Y, Wang FP (2009) Thermoelectric properties of Gd, Y co-doped  $\text{Ca}_3\text{Co}_4\text{O}_{9+\delta}$ . *Current Applied Physics* 9 (2):409-413. doi:10.1016/j.cap.2008.03.010
15. Rezaei M, Khajenoori M, Nematollahi B (2011) Preparation of nanocrystalline MgO by surfactant assisted precipitation method. *Materials Research Bulletin* 46 (10):1632-1637. doi:10.1016/j.materresbull.2011.06.007